Adsorption and catalytic oxidation of organic pollutants using Fe-zeolite

Analia V. Russo, Cesar Velasco Andrade, Laura E. De Angelis and Silvia E. Jacobo

ABSTRACT

In this work, a natural zeolite, modified and loaded with iron (NZ-A-Fe) as a heterogeneous catalyst, was characterized for its suitability as a permeable reactive barrier (PRB) material for treatment of aromatic hydrocarbons in groundwater. Adsorption and oxidation processes were analyzed. Batch adsorption tests for benzene, toluene and xylene (BTX) aqueous concentrated solutions were performed at neutral pH. Kinetic adsorption was described with the pseudo-second-order model. Experiments were performed using a stirred batch reactor with near 11 mM initial BTX concentration applying NZ-A-Fe as solid catalyst and H_2O_2 as an oxidant. BTX removal reached 80% in 600 min in these experimental conditions. Catalytic oxidation was described with a pseudo-first-order kinetic model. No significant iron leaching was detected during all the experiences. These investigations show that coupling adsorption with catalytic oxidation with this novel system is a promising procedure to simultaneously remove BTX from moderately concentrated aqueous solution at neutral pH in groundwater.

Key words | adsorption, BTX, catalyst, Fenton-like, water remediation, zeolites

Analia V. Russo
Cesar Velasco Andrade
Silvia E. Jacobo (corresponding author)
División Química de Materiales Magnéticos de aplicación en Ingeniería, Dpto Química, INTECIN Facultad de Ingeniería,
Universidad de Buenos Aires,
Av. Paseo Colón 850 (C1063ACV), Buenos Aires, Argentina
E-mail: *silviajacobo@gmail.com*

Laura E. De Angelis
Prof. Adjunta – Dpto. de Ingeniería Química
Instituto Tecnológico de Buenos Aires (ITBA),
(54911) 2150-4800 int. 5875
Av. Eduardo Madero 399,
Buenos Aires, Argentina

INTRODUCTION

BTEX (benzene, toluene, ethylbenzene and xylene) are widespread contaminants of groundwater and soils. These volatile and water soluble chemicals may be dispersed in the environment because of accidents and storage tank leakages (Kao *et al.* 2006).

The physicochemical properties of the fuel oxygenate make difficult their treatment with conventional water cleaning technologies (Sutherland *et al.* 2004) so it is still necessary to explore different and new techniques. Adsorption process in heterogeneous phase is an economically feasible process in the removing of different classes of pollutants from water and wastewater particularly in low concentrations. The need for an alternative low-cost easily available adsorbent has encouraged the search for new adsorbents as zeolites, as an option of solid structure. They possess three basic properties: ion exchange, adsorption and molecular sieving. These properties are exploited in a wide spectrum of applications, with a global market of several million tons per year. A significant number of studies have suggested that the area of application could be expanded by functionalization of the zeolite surface. Surfactant-modified zeolites (SMZs) have been described as highly effective for adsorption in the treatment of hydrocarbon-containing wastewater, although evidencing progressive surfactant release (with negative impact both on economics and environmental protection) (Altare *et al.* 2007; Schick *et al.* 2011).

Advanced oxidation processes are a group of processes that are based on the generation of highly reactive radicals, especially hydroxyl radicals ($OH^{\bullet}$), which are extremely active and nonselective oxidants, being able to oxidize a wide range of compounds that, otherwise, can be difficult to degrade. The Fenton's reagent ($H_2O_2 + Fe^{2+}$) has been used to treat wastewaters containing contaminants used in industrial practices (Kang & Hoffman 1998; Neyens & Baeyens 2009; Botas *et al.* 2010). Oxidation by the Fenton's reagent is traditionally represented by Equation (1). Ferric ions produced in reaction (1) can then react with H_2O_2

doi: 10.2166/wst.2017.611

to produce hydroperoxyl radicals ($HO_2^{\bullet}$) and restore ferrous ions (Equation (2)).

$$H_2O_2(ac) + Fe^{2+}(ac) \Rightarrow Fe^{3+}(ac) + OH^{\circ}(ac) + OH^{-}(ac) + HEAT \quad (1)$$

$$H_2O_2(ac) + Fe^{3+}(ac) \Rightarrow Fe^{2+}(ac) + H^{+}(ac) + HO_2^{\circ}(ac) \quad (2)$$

The hydroxyl radical ($OH^{\bullet}$) is a nonselective oxidant and it can mineralize an organic compound as:

$$C_xH_y(ac) + OH^{\circ}(ac) \Rightarrow CO_2(g) + H_2O(l) + HEAT \quad (3)$$

where C_xH_y is a generic organic compound.

However, it should be pointed out that classical Fenton's reagent, which is called as 'homogeneous Fenton process', leads to some significant problems related to the catalyst losses and its regeneration.

To overcome these drawbacks of homogeneous Fenton process, heterogeneous catalysts in which iron is located in the porous solid structure, have been developed. So, heterogeneous Fenton processes have been improved as a more practical and economical alternative to homogeneous Fenton process (Deng *et al.* 2008; Santos *et al.* 2010; Dükkancı *et al.* 2010). Nairat *et al.* (2015) reported the preparation of composite sorbents with iron nanoparticles and clinoptilolite for the removal of dyes, while Bayat *et al.* (2012) dispersed metallic clusters of iron in clinoptilolite as a catalyst for phenol degradation (initial phenol concentration: 100 mg/L and pH = 3.5) with good results. We have earlier reported (Russo *et al.* 2014) auspicious results for benzene removal with Fenton system at low pH, with iron nanoparticles inserted into a raw clinoptilolite (NZ-Fe). In these experiences we observed adsorption and degradation processes. Few researchers reported interesting results of organic pollutants removal (elimination) at neutral pH. Gamal *et al.* (2014) *et al.* employed ultrasonic-assisted heterogeneous Fenton reaction, using nanosized oxides of Cu and Fe, for nitrobenzene (NB) degradation where sonication played an important role in order to avoid iron precipitation.

Eun-Ju Kim *et al.* (2016) proposed, for wastewater treatment, manganese oxide nanorods for neutral Fenton conditions as more efficient catalysts.

In this work, the porous structure of a modified natural clinoptilolite as a supported catalyst (NZ-A-Fe) has been investigated to explore the behavior of this material in adsorption and oxidation processes. All the experiments were performed with relatively high concentrated benzene, toluene and xylene (BTX) aqueous solutions (near solubility) and at neutral pH, in order to explore the suitability of this material as a permeable reactive barrier (PBR) material for aromatic hydrocarbons treatment in groundwater.

EXPERIMENTAL

Materials and methods

Benzene (Bz) was purchased from Merck Química, toluene (Tol) was obtained from Biopack Chemical and *p*-xylene (Xyl) were obtained from Carboclor SA.

Two stock BTX-contaminated groundwater, with different concentrations (a and b), were prepared. They were obtained by adding the required volume (μl) of Bz, Tol and Xyl into a buffered solution to maintain pH = 7 during all the experiences.

(a) The absorption experiments were carried out using a batch operation mode with a stock solution with 1.3 mM in each component (2.3.2).
(b) For adsorption kinetic experiments with further oxidation course, a stock solution containing 5 mM Bz, 4.9 mM tol and 1.8 mM of Xyl. was prepared.

The buffer solution was prepared adding the adequate amounts of Na_2HPO_4 and NaH_2PO_4 in deionized water. The neck of the flask containing the stock solution was sealed with Teflon tape and it was stirred for 24 h to complete dissolving of the organic compounds.

The concentration of freely dissolved BTX was determined by gas chromatography (GC) analysis. Iron leaching was analyzed using an atomic absorption spectrometer instrument. Temperature was fixed at 20°C for all the experiences.

Preparation of Fe-loaded zeolite (NZ-A-Fe)

Natural clinoptilolite (NZ) was obtained from La Rioja (Argentina) through Diatec S.R.L. Structural characteristics were reported earlier (Russo *et al.* 2014, 2015a, 2015b). Cation capacity, iron content and particle size of the explored samples are presented in Table 1.

As it was earlier described, samples of this natural zeolite (NZ) were sieved and treated in NH_4Cl 3 M at 353 K during 8 h (sample NZ-A). Later, these samples were batch-loaded with iron salts (Fe(II)) and chemically reduced with sodium borohydride in order to prepare NZ-A-Fe.

Table 1 | Characteristics of the natural clinoptilolite (NZ) and of the iron loaded treated clinoptilolite (NZ-A-Fe)

Zeolite	MEC (meq/g)	EEC (meq/g)	Particle size (mm)	Fe content % w/w
NZ	1.82 ± 0.06	0.45 ± 0.03	0.3–0.5	1.4
NZ-A-Fe	–	0.47 ± 0.03	0.3–0.4	2.1

MEC, maximum experimental exchange capacity; EEC, external cation capacity.

Diffraction patterns and scanning electron microscopy (SEM) images of samples NZ, NZ-A and NZ-A-Fe were presented and discussed in our previous work (Russo *et al.* 2014, 2015a, 2015b).

Adsorption isotherms

Adsorption–desorption isotherms of NZ and the products from chemical and thermal treatments (NZ-A and NZ-A-Fe) were obtained by N_2 gas adsorption using a Coulter SA3100 surface area analyzer. Samples were outgassed overnight at 140 °C under vacuum for 3.0 h to attain a constant weight. The specific surface area (Brunauer–Emmett–Teller (BET)) was calculated by the BET method. V_{tot} was then evaluated by converting the volume of nitrogen adsorbed at p/ps ≈ 0.98 to the volume of liquid adsorbate, while pore size distribution was determined from desorption branch of the isotherms by Barrett–Joyner–Halenda method (BJH). The t-plot method has been used to calculate the microspore volume.

The equilibrium sorption isotherm in aqueous solution

The equilibrium sorption isotherm in aqueous solution, were measured at 20 ± 2 °C. 20 ml suspension samples with various BTX dilutions (1.3; 1.0; 0.8 and 0.5 mM) with 1.2 g NZ-A-Fe were arranged. A mixing time of 24 hours on a horizontal shaker was sufficient to reach the adsorption equilibrium. Samples were analyzed as 2.1

The BTX uptake at equilibrium (mg/g) was calculated by Equation (4).

$$q_e = \frac{(C_o - C_e)}{m}.V \quad (4)$$

where C_0 and C_e (mg/L) are the liquid-phase concentrations of BTX at the initial and at the equilibrium phase, respectively. V is the volume of the solution (L) and m is the mass of dry adsorbent used (g)

Sorption kinetics

60-mL glass vials with screw caps with septum were used to carry out kinetic experiences BTX sample of stock solution (2.1b) were placed into the vial in contact with 3.6 g of NZ-A-Fe. The vials were placed on a horizontal shaker and aliquot of 1 ml were extracted at prefixed time. All adsorption tests were performed in duplicate and the averages are reported.

Heterogeneous Fenton reaction

Samples (from BTX stock solution 2.1b) were mixed on a horizontal shaker for 24 hours in order to reach the absorption equilibrium. After this period, 3 ml of hydrogen peroxide (30% w/w), was added. Samples were mixed on a horizontal shaker while aliquots of 1 ml were extracted at different times. The concentration of freely dissolved BTX was determined by GC analysis. Temperature was fixed at 20 °C for all the experiences.

RESULTS AND DISCUSSION

Adsorption behavior of prepared samples

Important information about surface and porosity can be obtained from the adsorption-desorption isotherms as they can show the kind of porosity present in the samples. According to some results of structural investigations, clinoptilolite is characterized as a mineral adsorbent with two types of porosities such as primary porosity presented as a microporous structure (Hernández Huesca *et al.* 2016) and a secondary one formed by meso- and macrospores. A high value of total mesoporous volume on polymodal pore size distribution was obtained by many researchers using adsorption methods on natural clinoptilolite (Koruna *et al.* 2006; Sprynsky *et al.* 2010).

The nitrogen adsorption/desorption isotherms for NZ and for NZ-A-Fe treatment clinoptilolite are shown in Figure 1(a) and 1(c) respectively, while pore size distribution for both zeolites samples are presented in Figure 1(b) and 1(d).

Figure 1(a) and 1(c) show that low temperature nitrogen adsorption-desorption on both clinoptilolite samples are expressed by Isotherm of IV type by BDDT classification with the hysteresis loop of the type H4 (Figure 1(a) and 1(c)) according to IUPAC classification (IUPAC 1985). The isotherm curve rises too sharply at the beginning at a slight relative pressure ($P/P_0 < 0.02$) related to the presence of

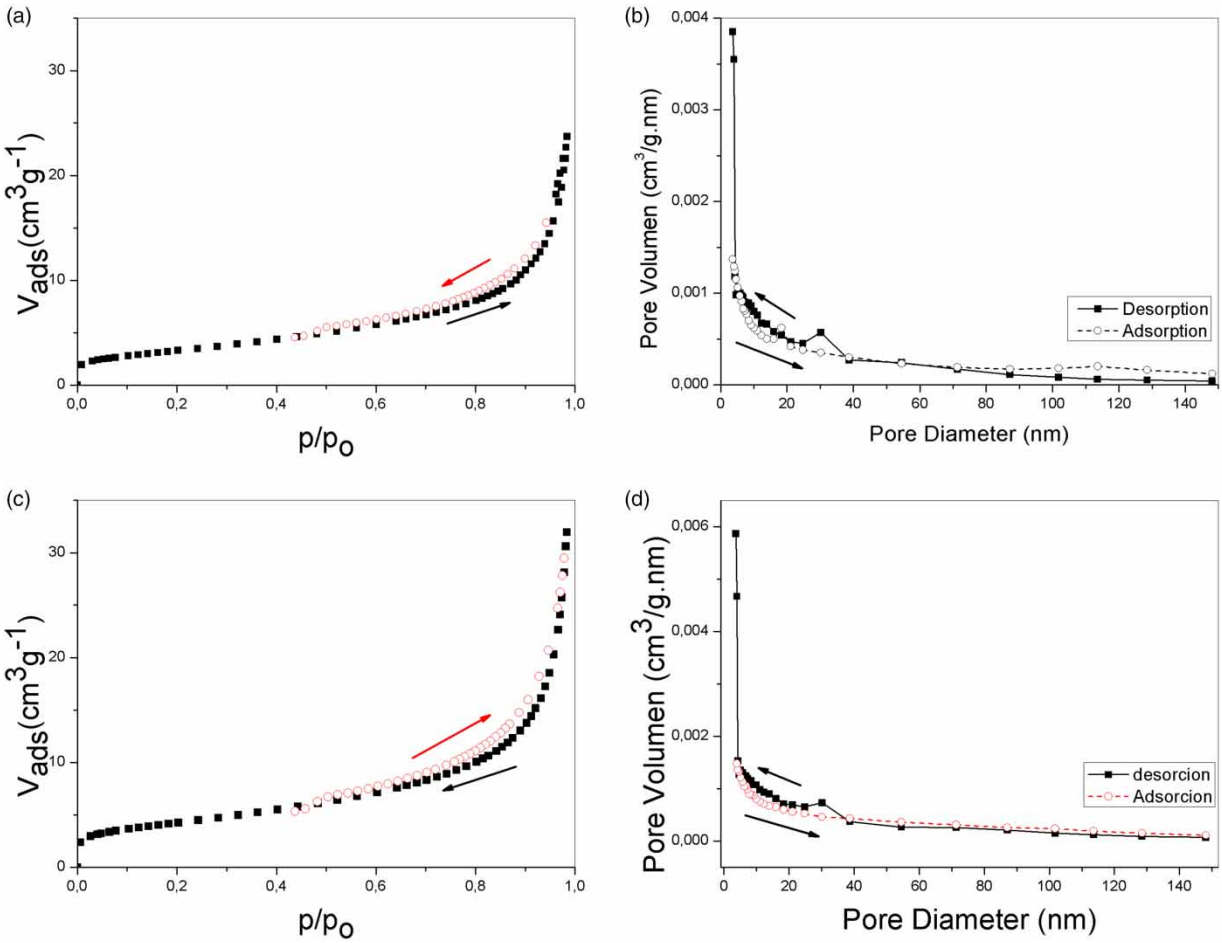

Figure 1 | (a) Nitrogen adsorption/desorption isotherms for the sample NZ. (b) Pore size distribution by BJH model for the sample NZ. (c) Nitrogen adsorption/desorption isotherms for the sample NZ-A-Fe. (d) Pore size distribution by BJH model for the sample NZ-A-Fe.

microspores (d < 6 nm). The hysteresis loop begins at the relative pressure near 0.43 for both presented samples. The microspore volume values for raw, natural zeolite (NZ) and for the iron loaded sample (NZ-A-Fe) determined by Saito–Foley (SF) model and calculated by t-plot are presented in Table 2 showing low values (0.0021 and 0.0017 cm^3/g, respectively) for both samples. The mesoporous volume, determined by BHJ model, show that the ammonium treatment followed by iron lodging decreases zeolite porosity (Table 2). The experimental porous volume values for this raw clinoptilolite (NZ) are similar to those reported by M. Sprynsky *et al.* for a clinoptilolite sample obtained from the Transcarpathian region in Ukraine (Sprynsky *et al.* 2010). Table 1 shows that iron content increases up to 50% in NZ-A-Fe compared to NZ, while the surface area decreases to a value of 9.78 m^2/g mainly due to the presence on iron nanoparticles (17% lower than the surface area of NZ) while the pore volume slightly decreases (in 7% see Table 2).

Table 2 | Parameters of the clinoptilolite porous structures by the nitrogen adsorption/desorption method

	Specific surface area ($m^2 \cdot g^{-1}$)		Pore volume ($cm^3 \cdot g^{-1}$)			Average pore diameter (nm)	
	S_{BET}	S_{BJH}	V_{tot} (BET)	V_{mes} (BJH)	V_{mic} (t – plot)	$D_{(BJH)}$	
NZ	11.85	10.61	0.0365	0.0344	0.0021	5.2	18.2
NZ-A-Fe	9.78	9.61	0.0345	0.0327	0.0017	5.2	29.7

Sorption isotherms

The relationships between adsorbent and adsorbate concentration at equilibrium phase can be described by sorption isotherms. The Langmuir and the Freundlich models are

the most frequently used. The Langmuir isotherm assumes monolayer coverage on a homogeneous surface with identical adsorption sites. In solution-solid systems, the isotherm adequacy can be seriously affected by the experimental conditions, in particular, the range of concentration of the solute/adsorbate.

The Freundlich isotherm is introduced as an empirical model,

$$q_e = K_f\ C_e^{1/n} \tag{5}$$

where q_e represents the amount adsorbed per amount of adsorbent at the equilibrium (mg/g), *Ce* represents the equilibrium concentration (mg/L), *1/n* and *Kf* are parameters that depend on the adsorbate and adsorbent.

Although Langmuir and Freundlich models were explored in this work, the experimental data, results revealed that Freundlich adsorption isotherm was the best model to fit the experimental values obtained for the adsorption of BTX onto NZ-A-Fe (Figure 2(a)).

Linearizing the Equation (5) results in the following expression:

$$\log(qe) = \log(Kf) + \frac{1}{n}\log(Ce) \tag{6}$$

where K_f and n are Freundlich constants which correspond to adsorption capacity and adsorption intensity, respectively. Figure 2(b) shows Freundlich isotherm representing the variation *log qe* with respect to *log Ce* for BTX adsorption onto NZ-A-Fe.

The n value indicates the degree of nonlinearity between solution concentration and adsorption. $n = 1$, indicates linear adsorption; $n < 1$, indicates a chemical process while $n > 1$, indicates a physical process. Table 3 shows that the n values in Freundlich equation varies from 0.7 to 0.9, (Table 3) which shows a cooperative adsorption.

Low *Kf* values are related to the low adsorption capacity of this clinoptilolite, probably as a consequence of its structurally small SiO_2/Al_2O_3 ratio (near 4.3) related to hydrophobicity. Table 3 shows that *Kf* Tol > *Kf* Bz in agreement with the maximum sorption behavior of Tol on NZ-A-Fe (Table 4).

Seifi *et al.* (2011) reported higher values for *Kf* in the sequence Bz > Tol > Xyl for BTX on modified ZSM-5 while adsorption values reported by Ghiachi *et al.* (2004) for benzene on modified ZSM-5-88, with ratio $31 < SiO_2/Al_2O_3 < 88$, were higher than our experimental results.

Sorption kinetics

Figure 3 shows the course of sorbed BTX fraction on NZ-A-Fe in the experiments for 1,800 min. BTX sorption process closely approached equilibrium within 100 min (inset Figure 3). No significant changes were observed from 120 to 1,600 min. The maximum adsorbed fraction (q_t) for Bz, Tol and Xyl were 2.7, 3.2 and 1.3 mg/g NZ-A-Fe, respectively. These q_t are in rich agreement with the K_f order obtained in Table 3 for these pollutants.

The pseudo-first-order and pseudo-second-order kinetics models were applied to analyze the kinetic and adsorption results.

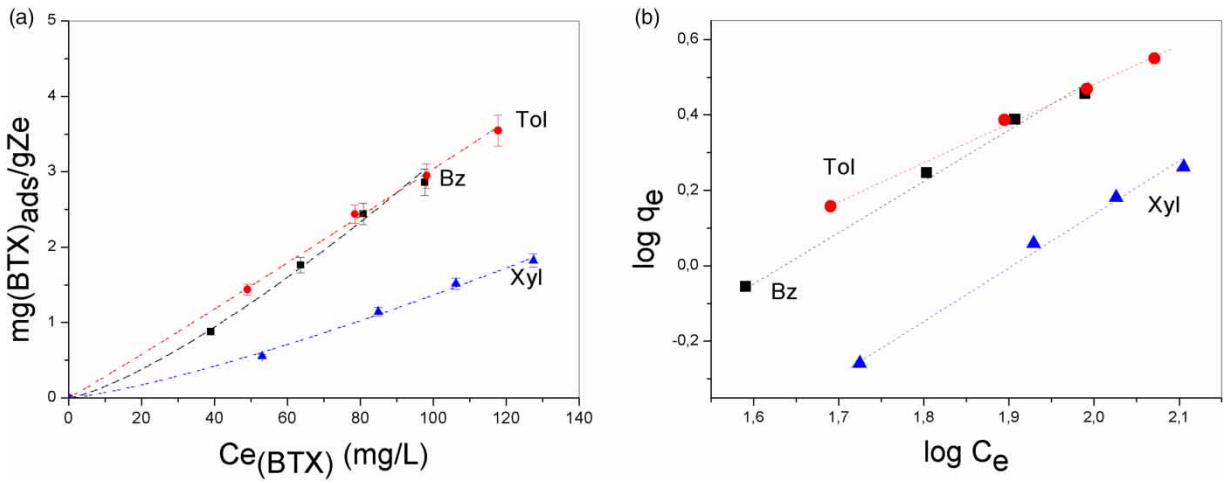

Figure 2 | (a) Adsorption isotherm of BTX for Ze-Fe (1.2 g de Ze-Fe, 20 mL solution BTX, 20 °C). (b) Freundlich isotherm representing variation log q_e with respect to log C_e for adsorption of BTX onto NZ-A-Fe.

Table 3 | Isotherms (Freundlich) parameters results for adsorption of BTX onto NZ-A-Fe

Parameters	Bz	Tol	Xil
K_f (mg/g)(L/mg)$^{1/n}$	0.0073	0.0266	0.0023
1/n	1.3143	1.02833	1.3856
n	0.761	0.972	0.722
R^2	0.98981	0.9955	0.9891

Table 4 | Pseudo-second-order model for adsorption BTX on ZN-A-Fe for an initial concentration of 5 mM (Bz), 4.9 mM (Tol) and 1.8 mM (Xyl) at pH = 7 and 20 °C

	$q_{e\ calc}$ (mg/g)	k_2 (g/mg·min)	R^2	Δq_t(%)
Bz	3.10	$6.03*10^{-3}$	0.9871	4.46
Tol	3.24	$12.1*10^{-3}$	0.9863	~0
Xyl	1.31	$57.5*10^{-3}$	0.9816	~0

Δq_t(%): normalized standard deviation.

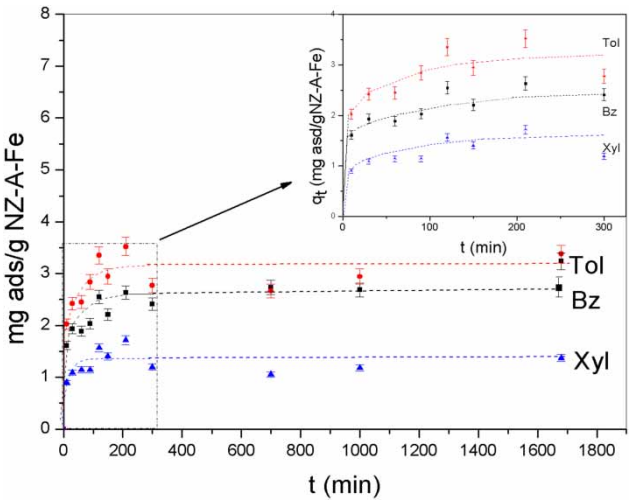

Figure 3 | Sorbed fraction (q_t) of BTX on NZ-A-Fe for an initial concentration of 5 mM (Bz), 4.9 mM (Tol) and 1.8 mM (Xyl) at pH = 7 and 20 °C.

(a) The pseudo-first-order kinetic model given by Langergreen and Svenska is defined as:

$$\ln(q_e - q_t) = \ln - (q_e) - k_1.t \quad (7)$$

where q_e and q_t are the mg the pollutant adsorbed at equilibrium and at any time (min), respectively. This model was discarded as neither the plot of ln $(q_e - q_t)$ vs time followed a linear behavior (not shown) nor the calculated parameters agreed with the experimental values.

(b) The pseudo-second-order kinetic model is expressed as:

$$\left(\frac{t}{q_t}\right) = \left(\frac{1}{k_2\, q_e^2}\right) + \left(\frac{t}{q_e}\right) \quad (8)$$

where k_2 (g mg^{-1} min) is the rate constant of second-order adsorption. The linear plot (Figure 4) showed a good agreement between the experimental and the calculated q_e values (Table 4) with good correlation coefficient values for the explored concentration presented in this work.

As it can be observed in Table 4, the rate constant of the second-order adsorption, k_2 is Xyl > Tol > Bz, which indicates that the uptakes decreased with water solubility and increased with molecular weight. The reported order of uptakes on SMZ, on the other hand, was Bz > Tol > Xyl (Torabian *et al.* 2010). This was due to the partition mechanism, which was reversely proportional to the octanol-water partition coefficients of BTEX, where the values of B, T, E, and X were 2.13, 2.69, 3.15, and 3.15–3.20, respectively. Therefore, our explored clinoptilolite (NZ-A-Fe) could be defined as material with a moderate adsorption capacity for low water solubility compounds with high molecular weight. The q_e calculated for each pollutant is related to the amount dissolved in the aqueous phase and these values are closed to the experimental data (Figure 3) for Tol and Xyl but higher for experimental Bz data (Figure 3). Notwithstanding, the normalized standard deviation Δq_t(%) shows relative low values (Table 4) compared to reported data by Tan *et al.* (2009). These results confirm that the pseudo-second-order kinetic model is suitable to describe the absorption kinetics.

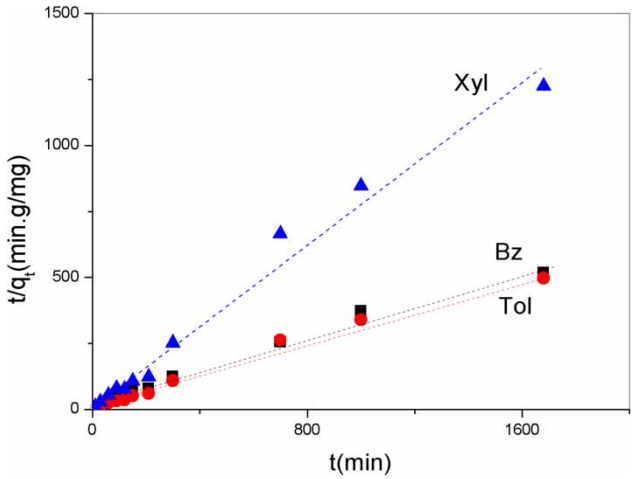

Figure 4 | Pseudo-second-order kinetics for adsorption BTX on ZN-A-Fe at pH = 7 and 20 °C.

In order to identify the adsorption mechanism, the intraparticle diffusion model proposed by Weber & Morris is tasted. (1963). It is an empirically found functional relationship where the adsorption fraction (q_t) varies proportionally to a function of $t^{1/2}$

$$q_t = k_{pi} t^{1/2} + C_i \quad (9)$$

The initial rate of intraparticle diffusion can be obtained by linearization of the curve $q_t = \mathrm{f}\,(t^{1/2})$ where k_{pi} is the kinetic parameter of stage i) and gives an idea about the thickness of the boundary layer. The plot q_t vs $t^{1/2}$ is related to the mechanism involved in the adsorption process. Only if the line passes through the origin, it would be possible to accept that the intraparticle diffusion is the only rate limiting process in the explored time.

Figure 5 shows that, for near the first three hours, two different processes that can be involved. The first sharper region up to 10 min can be attributed to an external surface adsorption (K_{pt1}) while the second section where a linear behavior is observed can be related to a gradual adsorption stage where intraparticle diffusion is rate-controlled (K_{pt2}). All these processes are close dependent on the pollutants initial concentration as it was reported by Tan *et al.* (2009) for the trichlorophenol absorption on activated carbon.

The experimental values for the kinetic data obtained from Figure 5 are presented in Table 5. It can be noticed that K_{pt2} shows lower values than the corresponding to the first stage (K_{pt1}) as each stage is the result of different mechanism. The values of K_{pt2} are lower than those reported for 2,4,6-trichlorophenol for Tan *et al.* (2009) for the adsorption of an organic pollutant on activated carbon. These results can be related to the different nature and morphology of the adsorbate. Seifi *et al.* (2011) reported lower K_{pt1} and K_{pt2} values for the adsorption of diluted BTX aqueous solutions on surfactant-modified granulated zeolites.

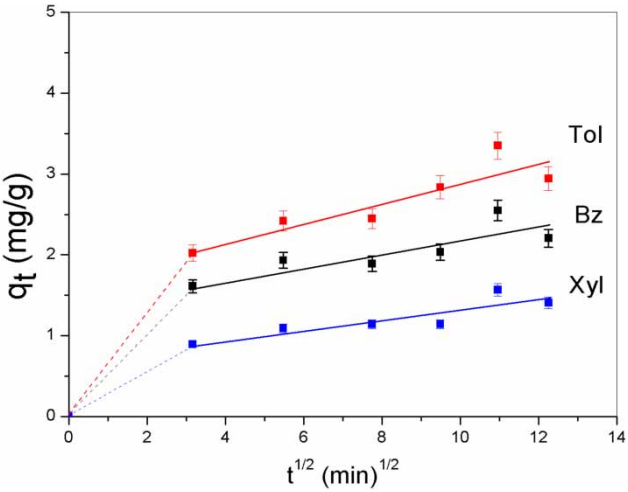

Figure 5 | Plot of intraparticle diffusion model for adsorption fraction q_t of BTX on NZ-A-Fe zeolite at 20 °C.

Table 5 | Intraparticle diffusion model constants and correlation coefficients for adsorption of BTX on NZ-A-Fe zeolite at 20 °C

	Intraparticle diffusion model				
BTX (mg/L)	K_{pt1} (mg/g min$^{1/2}$)	K_{pt2} (mg/g min$^{1/2}$)	C_1 (mg/g)	C_2 (mg/g)	$(R_2)^2$
Bz	0.492	0.084	0	1.358	0.776
Tol	0.643	0.128	0	1.632	0.857
Xyl	0.274	0.069	0	0.654	0.833

The intraparticle diffusion model fits the experimental results for the explored concentrations of the pollutants (BTX) for a relatively long time interval.

Heterogeneous Fenton reaction

Coupling adsorption with catalytic oxidation at neutral pH was motivated by the following reasons: (i) to reduce the reagents consumption, (ii) to avoid iron releasing during all the process and (iii) to improve the pollutant and catalyst contact during the adsorption process.

Heterogeneous Fenton reaction begun after the hydrogen peroxide was introduced into the reaction system. Figure 6 shows the variation of the BTX ratio C/C_o in the aqueous solution as degradation progresses.

Figure 6(a) profiles for Bz, Tol and Xylene show similar shapes. Rapid decay of BTX was observed for the first 60 min, followed by slow removal as time progressed. Figure 6(b) shows the experimental kinetic data plotted in order to characterize the removal mechanism. The observed kinetic of degradation system was reasonably well fitted to a pseudo-first-order model:

$$lnC - lnC_o = -k_1 t \quad (10)$$

where C is the concentration of the compound at any time (t), C_o is the initial concentration after sorption process and k_1 is the pseudo-first-order rate constant.

In this period, BTX was removed from the solution by an oxidation reaction onto the zeolite surface where a high BTX presence is concentrated in contact with the catalyst (Fe). This phenomenon is related to the intraparticle diffusion model (Table 5) and is one of the parameters that control the removal process rate.

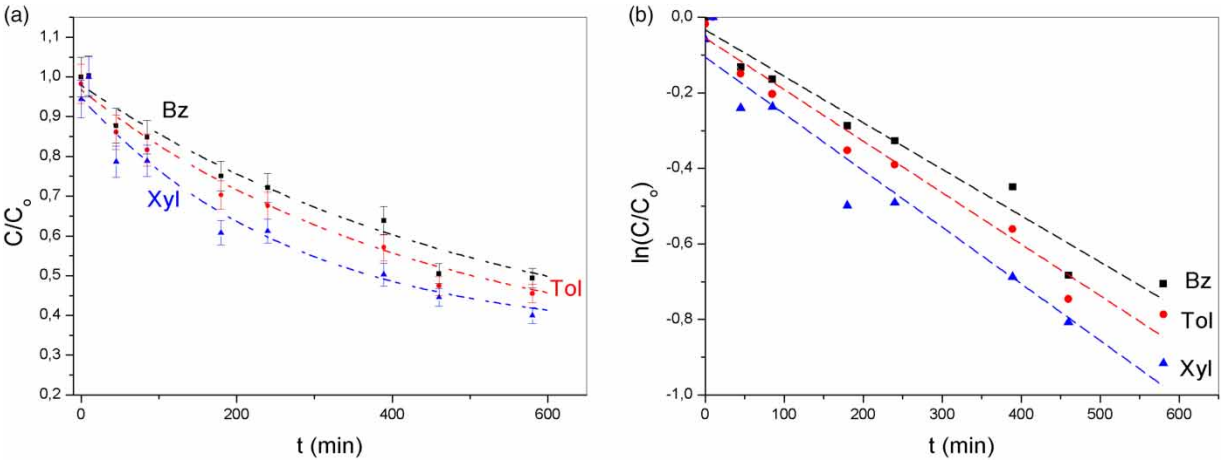

Figure 6 | Removal of BTX in an aqueous phase after sorption equilibrium was reached (a and b) pseudo-first order model for BTX removal ($Co_{Bz} = 5$ mM, $Co_{Tol} = 4.9$ mM, $Co_{Xil} = 1.8$ mM, with NZ-A-Fe $C_{Ze} = 60$ g/l, $C_{H2O2} = 0.44$ M = 15 g/l) pH = 7 and 20 °C.

Kinetic results (presented in Table 6) show that all the studied pollutants have similar kinetic behavior for the degradation process for the first (60 min) and second stage (600 min) in the order Xyl > Tol > Bz.

Adsorbed BTX is removed by oxidation and new BTX migrates from the aqueous solution into de zeolite. This assumption is supported by preliminary results where it was possible to observe that hydrogen peroxide concentration decreases continually when a zeolite sample, prepared as 2.4, is immersed in an hydrogen peroxide aqueous solution at pH = 7.

Solubilize iron remains below 0.15 ± 0.05 ppm during all the experiences. These results contribute to enhance the stability of the catalyst NZ-Fe prepared in this work. Such a low extend of release may be regarded as the iron resistance to the leaching process.

Taking into account the high initial concentration of BTX (near 65 mg) in contact with 3.6 g de catalyst (NZ-A-Fe), BTX removal reaches up to 80% in 600 min (near 15 mg BTX/g zeolite). These are promising results for heterogeneous Fenton processes at neutral pH for soil remediation.

Table 6 | Rate constants (k_1) and correlation coefficients (R^2) for the first-order kinetic model at the experimental conditions for t = 60 min and for 600 min

	$t_o = 60$ min		$t = 600$ min	
	$k1 \times 10^{-3}$ (min^{-1})	R^2	$k1 \times 10^{-3}$ (min^{-1})	R^2
Bz	2.5	0.9810	1.2	0.9600
Tol	2.7	0.9800	1.3	0.9680
Xyl	2.9	0.9760	1.4	0.9454

($Co_{Bz} = 5$ mM, $Co_{Tol} = 4.9$ mM, $Co_{Xil} = 1.8$ mM, with NZ-A-Fe $C_{Ze} = 60$ g/l, $C_{H2O2} = 0.44$ M = 15 g/l) pH = 7 and 20 °C.

Further experiences are in progress in order to take knowledge about the internal mechanism associated to the degradation processes.

CONCLUSION

The adsorption and oxidation of BTX by a natural modified clinoptilolite (SiO_2/Al_2O_3 near 4.3), lodged with iron was investigated. BTX adsorption for diluted samples was best fitted by Freundlich equation while kinetic adsorption for high aqueous concentrated solutions was described with the pseudo-second-order kinetic model. The intraparticle diffusion scheme fits the experimental results for a relative long time interval.

In these experiments, NZ-A-Fe demonstrates a preliminary adsorption behavior while supports the catalyst for the oxidation Fenton-like reaction.

Based on the results of this study we conclude that coupling adsorption with catalytic oxidation is a promising system to remove different organic pollutant (BTX) from aqueous solution at neutral pH without leaching of iron species. In these experimental conditions, BTX removal was near 15 mg BTX/g NZ-A-Fe. New investigations are in process in order to determine the main parameters for the design of a PRB.

ACKNOWLEDGEMENTS

The authors thank Gustavo Panizza from DIATEC S.R.L. for zeolite provision. This project was partially funded by UBACyT (2014-2017).

REFERENCES

Altare, C. R., Bowman, R. S., Katz, L. E., Kinney, K. A. & Sullivan, E. J. 2007 Regeneration and long-term stability of surfactant-modified zeolite for removal of volatile organic compounds from produced water. *Microporous and Mesoporous Materials* **105**, 305–316.

Bayat, M., Sohrabi, M. & Javid Royaee, S. 2012 Degradation of phenol by heterogeneous Fenton reaction using Fe/clinoptilolite. *Journal of Industrial and Engineering Chemistry* **18**, 957–962.

Botas, J. A., Melero, J. A., Martinez, F. & Pariente, M. I. 2010 Assessment of Fe_2O_3/SiO_2 catalysts for the continuous treatment of phenol aqueous solutions in a fixed bed reactor. *Catalysis Today* **149**, 334–340.

Deng, J., Jiang, J., Zhang, Y., Lin, X., Du, C. & Xiong, Y. 2008 $FeVO_4$ as a highly active heterogeneous Fenton-like catalyst towards the degradation of Orange II. *Applied Catalysis B: Environmental* **84**, 468–473.

Dükkancı, M., Gündüz, G., Yılmaz, S., Yaman, Y. C., Prikhod'ko, R. V. & Stolyarova, I. V. 2010 Characterization and catalytic activity of CuFeZSM-5 catalysts for oxidative degradation of Rhodamine 6G in aqueous solutions. *Applied Catalysis B: Environmental* **95**, 270–278.

Gamal, M. S., ElShafei, F. Z., Yehia, O. I. H., Dimitry, A. M. & Eshaq Badawi, G. H. 2014 Ultrasonic assisted-Fenton-like degradation of nitrobenzene at neutral pH using nanosized oxides of Fe and Cu. *Ultrasonics Sonochemistry* **21** (4), 1358–1365.

Ghiaci, M., Abbaspur, A., Kia, R. & Seyedeyn-Azad, F. 2004 Equilibrium isotherm studies for the sorption of benzene, toluene, and phenol onto organo-zeolites and as-synthesized MCM-41. *Separation and Purification Technology* **40**, 217–229.

Hernández Huesca, R., Perez Arcos, J., Vargas Hernández, D. & Perez Cruz, M. A. 2016 Adsorption kinetics of N_2O on natural zeolites 2016. *Revista Internacional de Contaminación Ambiental* **32** (2), 237–242.

IUPAC Reporting Physisorption Data for Gas/Solid Systems with Special Reference to the Determination of Surface Area and Porosity 1985 Section 5. Evaluation of Adsorption Data. *Pure Applied Chemistry* **57**, 611–615.

Kang, J. & Hoffman, M. R. 1998 Kinetics and mechanism of the sonolytic destruction of methyl tert-butyl ether by ultrasonic irradiation in the presence of ozone. *Environmental Science & Technology* **32**, 3194–3199.

Kao, C. M., Huang, W. Y., Chang, L. J., Chen, T. Y., Chien, H. Y. & Hou, F. 2006 Application of monitored natural attenuation to remediate a petroleum-hydrocarbon spill site. *Water Science Technology* **53**, 321–328.

Kim, E.-J., Oh, D., Lee, C.-S., Gong, J., Kim, J. & & Chang, Y.-S. 2017 Manganese oxide nanorods as a robust Fenton-like catalyst at neutral pH: crystal phase-dependent behavior. *Catalysis Today* **282** (1), 71–76.

Koruna, O., Leboda, R. & Skubiszewski, R. 2006 Structural and physicochemical properties of natural zeolites: clinoptilolite and mordenite. *Microporous and Mesoporous Materials* **87**, 243–246.

Nairat, M., Shahwan, T., Eröglu, A. & Fuchs, H. 2015 Incorporation of iron nanoparticles into clinoptilolite and its application for the removal of cationic and anionic dyes. *J. Ind. Eng. Chem.* **21**, 1143–1151.

Neyens, E. & Baeyens, J. 2009 A review of thermal sludge pre-treatment processes to improve dewaterability. *Journal of Hazardous Materials* **98** (1–3), 33–50.

Russo, A. V., Toriggia, L. F. & Jacobo, S. E. 2014 Natural clinoptilolite zeolite loaded with iron for aromatic hydrocarbons removal from aqueous solutions. *Journal of Materials Science* **49** (2), 614–620.

Russo, A. V., Domé Lobo, D. N. & Jacobo, S. E. 2015a Removal of MTBE in column filled with modified natural zeolites. *Procedia Materials Science* **8**, 375–382.

Russo, A. V., Labourt, A., Bercoff, P. G. & Jacobo, S. E. 2015b Optimization of iron load in a natural zeolite for heterogeneous catalysis. *International Refereed Journal of Engineering and Science (IRJES)* **4** (4), 19–25.

Santos, A., Yustos, P., Rodriguez, S., Simon, E. & Romero, A. 2010 Fenton pretreatment in the catalytic wet oxidation of phenol. *Industrial & Engineering Chemistry Research* **49** (12), 5583–5587.

Schick, J., Caullet, P., Paillaud, J. L., Patarin, J. & Mangold Callarec, C. 2011 Nitrate sorption from water on a surfactant-modified zeolite. Fixed-bed column experiments *Microporous and Mesoporous Materials* **142** (2–3), 549–556.

Seifi, L., Torabian, A., Kazemian, H., Nabi Bidhendi, G., Akbar Azimi, A. & Charki, A. 2011 Adsorption of petroleum monoaromatics from aqueous solutions using granulated surface modified natural nanozeolites: systematic study of equilibrium isotherms. *Water, Air, & Soil Pollution* **217**, 611–625.

Sprynsky, M., Golembiewski, R., Trykowski, G. & Buszewski, B. 2010 Heterogeneity and hierarchy of clinoptilolite porosity. *Journal of Physics and Chemistry of Solids* **71**, 1269–1273.

Sutherland, J., Adams, C. & Kekobad, J. 2004 Treatment of MTBE by air stripping, carbon adsorption, and advanced oxidation: technical and economic comparison for five groundwaters. *Water Research* **38**, 193–205.

Tan, I. A. W., Ahmad, A. L. & Hameed, B. H. 2009 Adsorption isotherms, kinetics, thermodynamics and desorption studies of 2,4,6-trichlorophenol on oil palm empty fruit bunch-based activated carbon. *Journal of Hazardous Materials* **164**, 473–482.

Torabian, A., Kazemian, H., Seifi, L., Bidhendi, G. N., Azimi, A. A. & Ghadiri, S. K. 2010 Adsorption of BTEX on surfactant modified granulated natural zeolite nanoparticles: parameters optimizing by applying taguchi experimental design method. *Clean-Soil Air Water* **38**, 77–83.

Weber, W. J. & Morris, J. C. 1963 Kinetics of adsorption on carbon from solution. *Journal of the Sanitary Engineering Division* **89**, 31–60.

First received 21 September 2017; accepted in revised form 23 November 2017. Available online 7 December 2017